

Support Functionalization with a Phosphine-Containing Hyperbranched Polymer: A Strategy to Enhance Phosphine Grafting and Metal Loading in a Hydroformylation Catalyst

Marco A. S. Garcia,^[a] Rodrigo S. Heyder,^[a] Kelley C. B. Oliveira,^[b] Jean C. S. Costa,^[a] Paola Corio,^[a] Elena V. Gusevskaya,^[b] Eduardo N. dos Santos,^[b] Reinaldo C. Bazito,^[a] and Liane M. Rossi^{*[a]}

We present the design of a hydroformylation catalyst through the immobilization of air-stable Rh nanoparticles (NPs) on a magnetic support functionalized with a hyperbranched polymer that bears terminal phosphine groups. The catalyst modification with the hyperbranched polymer improved the metal-support interaction, the metal loading, and the catalytic activity. The catalyst was active for the hydroformylation of natural products, such as estragole, and could be used in successive

reactions with negligible metal leaching. The phosphine grafting played a key role in the recyclability of Rh NPs under hydroformylation conditions. The catalytic activity was maintained in successive reactions, even if the catalyst was exposed to air during each recovery procedure. The modification of the support with hyperbranched polyester allowed us either to increase the number of Rh active species or to obtain more active Rh species on the catalyst surface.

Introduction

The development of strategies for the immobilization of metal active phases and complexes on inorganic, organic, or hybrid supports, for example, magnetic nanomaterials,^[1] polymers,^[2] or supported ionic-liquid phases,^[3] for the production of easily recyclable catalysts is highly welcomed. The properties of a given material used as a catalyst support, for example, silica, can be tuned by the functionalization of its surface before the immobilization step, which allows a better interaction with the active phase precursors and avoids metal leaching or even the fine-tuning of its reactivity.^[4] Surface silanol groups are easy to functionalize by reacting the silica matrix with organoalkoxysilane reagents, but the number of reactive silanol groups on the silica surface somehow limits the number of terminal functional groups obtained. Several studies deal with the functionalization of supports for the preparation of supported catalysts; however, quite a few of them discuss the efficiency of

the functional-group grafting process or suggest strategies to enhance support functionalization. For example, the number of terminal functional groups can, in principle, be multiplied by increasing the support surface area or the grafting of hyperbranched polymers on the silica surface that can act as molecular linkers to the desired terminal functional groups.^[5]

Hyperbranched polymers are molecules composed of repeating units that arise from a central core characterized by at least two functionalities, from which multifunctional branched units are derived to form an irregular 3D dendritic globular structure. If all the units are attached perfectly into a highly ordered molecular structure, they are called dendrimers.^[6] Over the last few decades, hyperbranched polymers have received attention because of their potential application in many different areas, such as catalysis, electronics, optics, biology, medicine, and ecology.^[6,7] One of the advantages of hyperbranched polymers over dendrimers is their synthetic simplicity. They may be synthesized by the polymerization of an AB_n or a latent AB_n monomer (single-monomer methodology) or by the direct polymerization of two types of monomers (double-monomer methodology). These synthetic paths provide an irregular molecule with a broad molecular weight distribution that still possesses properties similar to those of dendrimers, such as low viscosity and high solubility.^[8]

Dendrimers and hyperbranched polymers have been used as platforms for the preparation of catalysts for various reactions. For example, Stephenson et al. used a Ni complex coordinated to a hyperbranched polymer microstructure to catalyze olefin polymerization.^[9] Nabae et al. have described the use of a solid sulfonic acid functionalized hyperbranched poly-

[a] M. A. S. Garcia, R. S. Heyder, Dr. J. C. S. Costa, Dr. P. Corio, Dr. R. C. Bazito, Dr. L. M. Rossi
Institute of Chemistry
University of São Paulo
Av. Prof. Lineu Prestes, 748
05508-000, São Paulo (Brazil)
E-mail: lrossi@iq.usp.br

[b] Dr. K. C. B. Oliveira, Dr. E. V. Gusevskaya, Dr. E. N. dos Santos
Chemistry Department
Federal University of Minas Gerais
Av. Antônio Carlos, 6627
31270-901 Belo Horizonte (Brazil)

Supporting Information and the ORCID identification number(s) for the author(s) of this article can be found under <http://dx.doi.org/10.1002/cctc.201600070>.

(ether sulfone) as a catalyst for the esterification of 1-butanol with acetic acid.^[10] Hyperbranched polymers have also been used in the design of catalytic systems for the hydroformylation reaction. Some of those applications are based on the possibility to prepare water-soluble catalysts to perform aqueous biphasic catalysis or improve their solubility in an organic medium.^[11] Several applications of Rh complexes attached to dendrimers in hydroformylation reactions have been described. Lu and Alper^[12] attributed the improvement of reactivity and selectivity to the cooperative catalytic behavior of the multiple coordination sites of the interior and exterior functional groups of Rh-containing dendrimers. Helms and Fréchet^[13] pointed out that the improved catalytic performance could be the result of a confinement effect of the substrate and the catalyst at the dendrimer–solvent interface to afford a high local concentration of reactive groups within a well-defined nanoscopic reaction volume. Rh-dendrimer complexes have been used as homogeneous catalysts in organic media,^[11b] in aqueous biphasic catalysis,^[11a] and after immobilization on solid supports.^[12,14]

In recent years, magnetic nanoparticles have been studied intensively as catalyst supports because of their magnetic properties,^[1] which include the preparation of magnetically recoverable hydroformylation catalysts. $[\text{Rh}(\text{cod})(\eta^6\text{-benzoic acid})\text{BF}_4]$ (cod = cyclooctadiene) was immobilized directly on the surface of ferrite nanoparticles through interaction with the carboxylic acid. The supported catalyst showed excellent catalytic activity and regioselectivity in hydroformylation reactions, which were comparable to those with the homogeneous counterpart. $[\text{Rh}(\text{cod})(\mu\text{-S}-(\text{CH}_2)_{10}\text{CO}_2\text{H})_2]$ was immobilized directly on the surface of ferrite nanoparticles through the carboxylic acid approach.^[15] Abu-Reziq et al. dendronized magnetic nanoparticles to prepare a magnetically recoverable hydroformylation catalyst.^[16] They prepared polyamidoamine (PAMAM) dendronized silica-coated magnetic nanoparticles up to the third generation using a two-step approach: the Michael addition of methyl acrylate with amine groups on the silica surface followed by amidation with ethylenediamine. The terminal amino groups were phosphonated with diphenylphosphinomethanol prepared in situ from diphenylphosphine and paraformaldehyde. The phosphonated magnetic nanomaterial was used for the immobilization of $[\text{Rh}(\text{cod})\text{Cl}]_2$ and applied in hydroformylation reactions.

Previously, we reported the preparation of a hydroformylation catalyst through the immobilization of Rh nanoparticles (NPs) on a magnetic support, the surface of which was functionalized with propylamino bis(methylenediphenylphosphine) ligands.^[17] The aminopropyl moiety grafted into the support surface (silica-coated magnetite) was phosphinomethylated to give terminal diphenylphosphine groups that interacted with Rh NPs. This interaction allowed the immobilization of catalytically active Rh species on the surface and prevented metal leaching under hydroformylation conditions. As an example, the concentration of the phosphine groups was 0.4 mmol g^{-1} and the metal loading was very low (0.2 wt% Rh). Herein, we explored the functionalization of a magnetic support with hyperbranched polyester with terminal amine groups and their

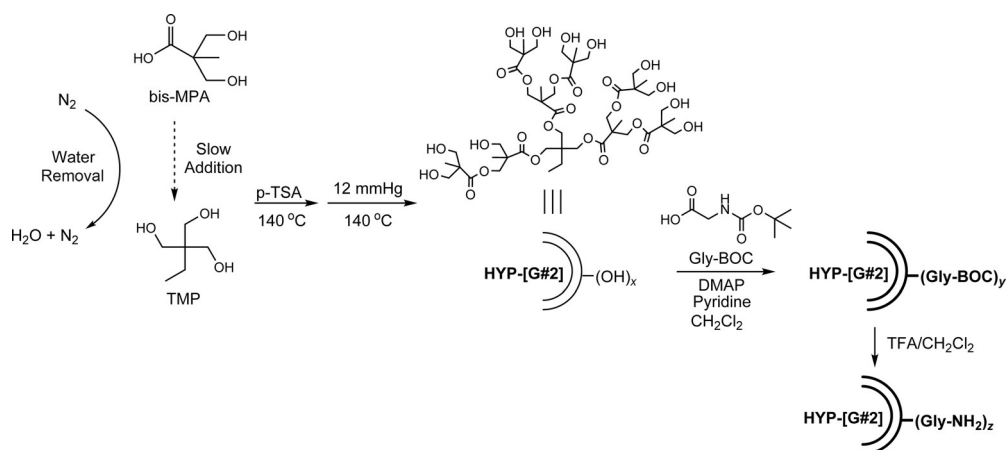
phosphomethylation to give terminal diphenylphosphine groups as a strategy for the preparation of a hydroformylation catalyst with enhanced phosphine grafting and a high metal loading. The catalytic performance of the material as well as its chemical and air stability were evaluated in the hydroformylation of natural products (in particular, estragole), a very important reaction in fine chemistry for the valorization of the components of bio-renewable essential oils.

Results and Discussion

The support functionalization with diphenylphosphine moieties played a key role in the recyclability of the Rh catalyst under hydroformylation conditions.^[17] The strategy used in our previous work was based on the condensation of (3-aminopropyl)triethoxysilane with the silica surface silanol groups followed by the phosphomethylation of the surface amino groups to produce bis(methylenediphenylphosphine) moieties $[\text{Fe}_3\text{O}_4@\text{SiO}_2\text{-N}(\text{CH}_2\text{PPh}_2)_2]$ with 0.4 mmol of PPh_2 per gram of the solid material. The Rh catalyst, $\text{Fe}_3\text{O}_4@\text{SiO}_2\text{-N}(\text{CH}_2\text{PPh}_2)_2\text{Rh}$, was then prepared by the impregnation of Rh NPs (synthesized through the sol immobilization method); however, the metal uptake obtained was quite low (0.2 wt% Rh). The impregnation process was repeated, but the metal loading was not improved, which revealed a weak metal–support interaction. Herein, we have used a hyperbranched ligand for the support functionalization step as a strategy to enhance the number of terminal phosphine groups.

A pseudo-second-generation hyperbranched polymer (HYP-[G#2]-(OH)₁₂) was synthesized using a pseudo-one-pot reaction described elsewhere.^[18] The –OH-terminated material was further modified by the conjugation of the amino acid glycine,^[12] which resulted in the presence of free amino groups (Scheme 1). The number of free amino groups was determined by using ¹H NMR spectroscopy (Figure 1) and confirmed by using MS (Figure S1). The reaction between the hyperbranched material with glycine-di-*tert*-butyl dicarbonate (BOC) results in the appearance of the peaks of the BOC group (p), the NH group (n), and the CH₂ group (m). The deprotection step left the free amine group, as shown by the disappearance of the peak of the BOC group. The integration of the peak of the core (a) compared with the CH₂ peak from the glycine molecule revealed 7.6 peripheral –NH₂ groups per molecule.

The amino-functionalized catalyst support $\text{Fe}_3\text{O}_4@\text{SiO}_2\text{-NH}_2$ was first subjected to a standard conjugation protocol with the cross-linking reagent glutaraldehyde^[19] for the covalent coupling of an amine group of the hyperbranched polyester to an amine group of the functionalized support through imine bonds.^[20] The envisaged functionalization steps are illustrated in Scheme 2. The peripheral amino groups were used to further functionalize the support with an organic moiety that possesses a terminal phosphine group. The phosphine moieties were introduced through the reaction of the terminal amino groups of the hyperbranched structures with paraformaldehyde and diphenylphosphine.^[17,21] The incorporation of organic ligands on the surface of the silica-coated magnetic material was evaluated by FTIR spectroscopy and thermogravimetric



Scheme 1. Synthesis of a pseudo-second-generation hyperbranched polymer with trimethylolpropane as the core and subsequent modification of the peripheral groups to result in HYP-[G#2]-(NH₂)_z.

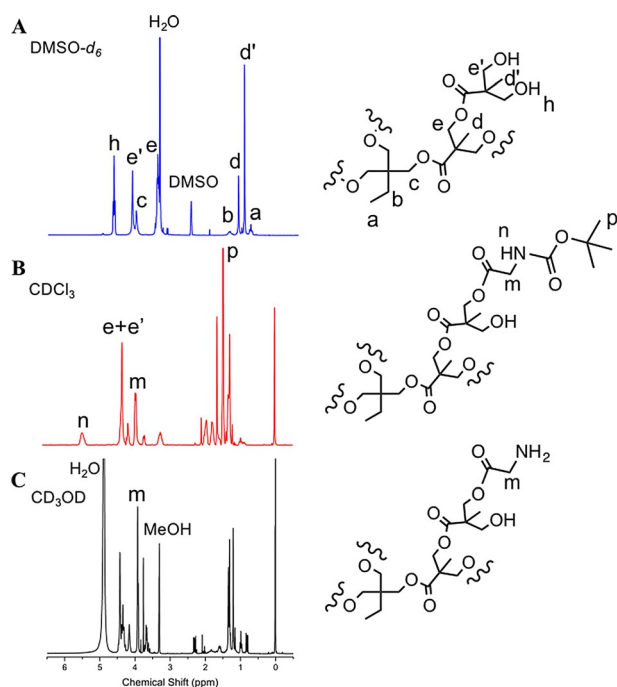
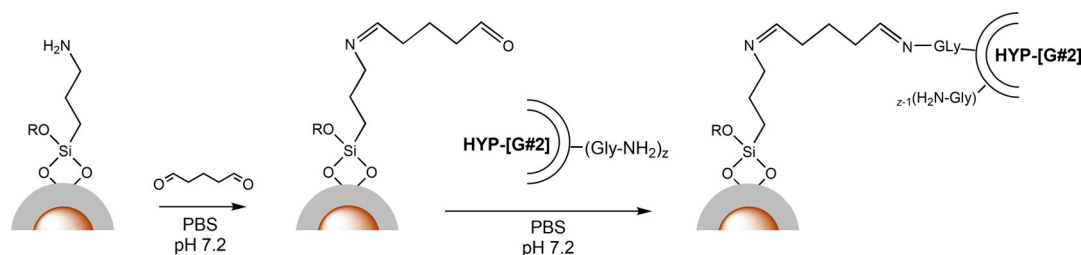
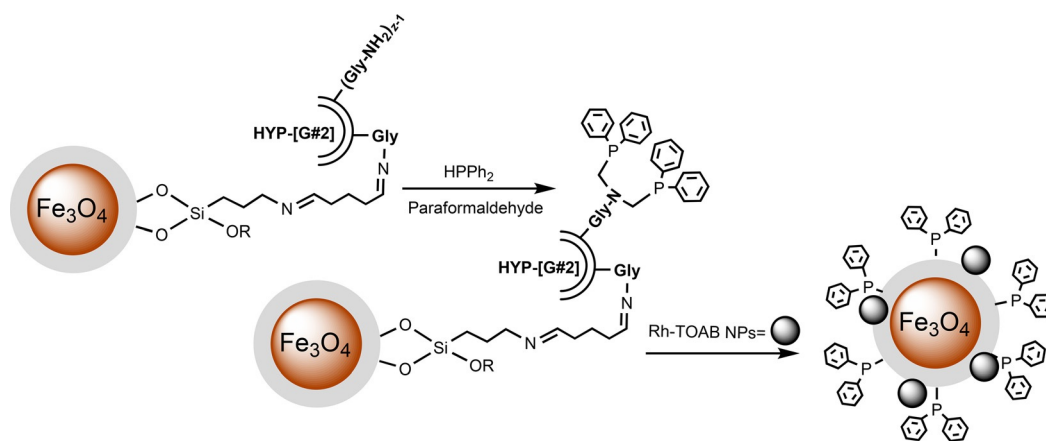


Figure 1. ¹H NMR spectra of A) HYP-[G#2]-(OH)₁₂, B) HYP-[G#2]-(Gly-BOC)_y, and C) HYP-[G#2]-(NH₂)_z. The deuterated solvent used is specified for each analysis, as well as peaks from water and residual solvents.

(TG) analysis (Figures S2 and S3). The FTIR spectrum of Fe₃O₄@SiO₂-NH₂ exhibits characteristic vibrational bands of silica and vibrational bands at $\tilde{\nu} = 2700\text{--}2900\text{ cm}^{-1}$ characteristic of the CH₂ stretching of aminopropyl groups. After reaction with glutaraldehyde, an increase of the relative intensity of the vibrational bands at $\tilde{\nu} = 2700\text{--}2900\text{ cm}^{-1}$ suggests the presence of more CH₂ groups.^[22] The stretching mode of the imine bond (N=CH–) and aldehyde (C=O) were not easy to distinguish from the existing silica bands and could not be assigned. The last two steps in the silica functionalization (Fe₃O₄@SiO₂-HYP-(NH₂)_z and Fe₃O₄@SiO₂-HYP-N(CH₂PPh₂)₂) do not lead to significant changes in the FTIR spectra, which are dominated by the vibrational modes of the silica matrix. These surface modifications; however, were evident in the analysis of the Raman spectra and will be discussed later. TG analysis provided further evidence for the successful modification of the silica surfaces. The weight loss below 100 °C caused by the loss of adsorbed water is present in all samples. Above 100 °C, the curves were different. The silica-coated magnetic material (Fe₃O₄@SiO₂) and the amine-modified material (Fe₃O₄@SiO₂-NH₂) showed roughly the same weight loss ($\approx 4.5\%$) above 100 °C. The weight loss of the materials modified with the hyperbranched polymer Fe₃O₄@SiO₂-HYP-NH₂ (23.8 %) and Fe₃O₄@SiO₂-HYP-N(CH₂PPh₂)₂ (25.7 %) was remarkably high, which suggests the successful covalent attachment of the hyperbranched polymer derivatives onto the silica surface. The



Scheme 2. Steps for the surface functionalization of Fe₃O₄@SiO₂.



Scheme 3. Rh-TOAB NPs immobilized onto the $\text{Fe}_3\text{O}_4@SiO_2\text{-HYP-N}(\text{CH}_2\text{PPh}_2)_2$ support.

proportion of phosphorus in the material determined by using inductively coupled plasma optical emission spectrometry (ICP-OES) was 2.3 wt%, which corresponded to 0.8 mmol of PPh_2 per gram of the solid material.

The Rh catalyst was prepared by the immobilization of Rh NPs stabilized with tetraoctylammonium bromide (TOAB) on the $\text{Fe}_3\text{O}_4@SiO_2\text{-HYP-N}(\text{CH}_2\text{PPh}_2)_2$ material (Scheme 3). The Rh NPs (2.5 ± 0.3 nm) were synthesized using a modification of the method described by Brust et al.^[23] as reported by us elsewhere.^[17,24] TEM images of the catalyst (Figure 2) revealed that

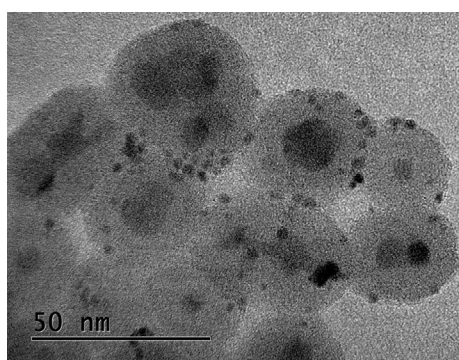


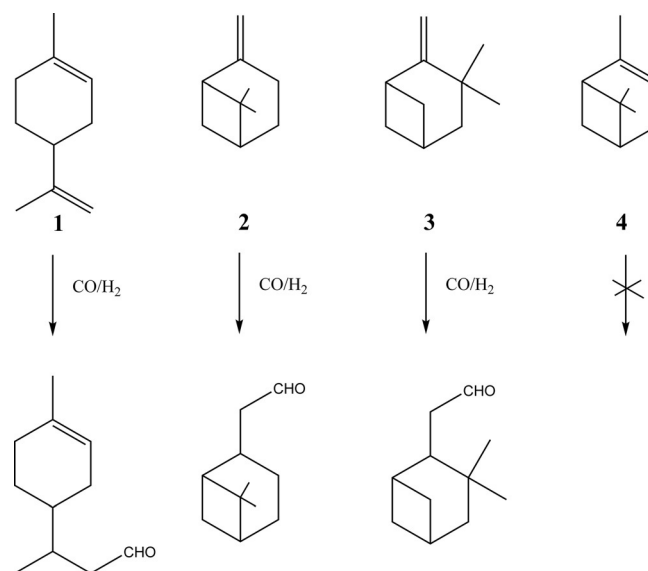
Figure 2. TEM image of $\text{Fe}_3\text{O}_4@SiO_2\text{-HYP-N}(\text{CH}_2\text{PPh}_2)_2\text{Rh}$.

the Rh-TOAB NPs are attached to the support surface and did not change in size after immobilization. The characterization of the free Rh-TOAB NPs is published elsewhere.^[24] The metal loading was determined by using flame atomic absorption spectrometry (FAAS) as 1.0 wt% Rh. Thus, the hyperbranched modified material, $\text{Fe}_3\text{O}_4@SiO_2\text{-HYP-N}(\text{CH}_2\text{PPh}_2)_2\text{Rh}$, bears twice as much phosphine and a five-times higher concentration of Rh on its surface than our $\text{Fe}_3\text{O}_4@SiO_2\text{-N}(\text{CH}_2\text{PPh}_2)_2\text{Rh}$ catalysts reported previously.^[17]

Our attempt to enhance the number of terminal phosphine groups and metal loading using a hyperbranched ligand was successful and represents an excellent strategy for the design of new hydroformylation catalysts. The increase in the metal uptake was not directly proportional to the concentration of

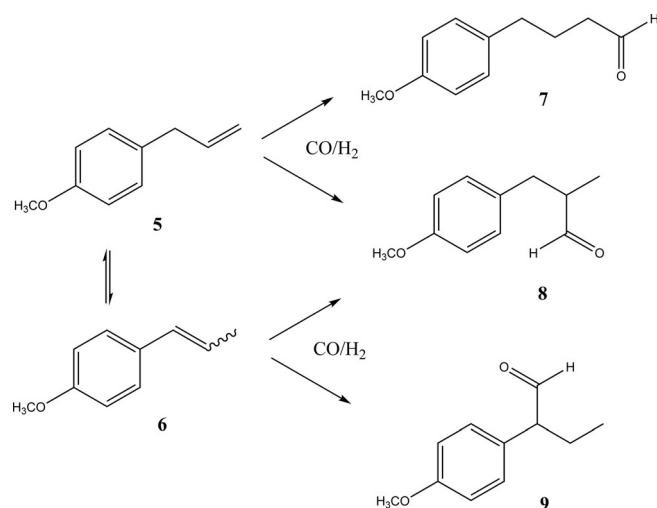
phosphine terminal groups; therefore, we can expect a contribution of the hyperbranched ligand on the immobilization process.

The catalytic properties of $\text{Fe}_3\text{O}_4@SiO_2\text{-HYP-N}(\text{CH}_2\text{PPh}_2)_2\text{Rh}$ were tested in the hydroformylation of several naturally occurring olefins. Initial screening was performed with three monoterpenes that have terminal disubstituted double bonds, that is, limonene (**1**), β -pinene (**2**), and camphene (**3**), α -pinene (**4**), a monoterpene with an endocyclic double bond, and estragole (**5**), an allylaromatic olefin with a terminal monosubstituted double bond (Schemes 4 and 5). All these substrates are available from essential oils of many plants and represent a green alternative source of renewable feedstocks for the flavor and fragrance industry.



Scheme 4. Hydroformylation of monoterpenes.

Under standard reaction conditions (40 atm, 80°C , substrate/Rh molar ratio of 2000, and 24 h), the olefins showed different reactivities towards hydroformylation (Table 1). As expected, the most reactive substrate was estragole (100% conversion)



Scheme 5. Hydroformylation of estragole.

Table 1. Hydroformylation of alkenes catalyzed by Fe₃O₄@SiO₂-HYP-N(CH₂PPh₂)₂Rh.^[a]

Entry	Substrate	Conversion [%]	Selectivity [%]		TOF ^[c] [h ⁻¹]
			Aldehydes	Isomers ^[b]	
1	limonene (1)	41	68	32	34
2	β-pinene (2)	56	27	73	47
3	camphene (3)	11	100	–	9
4	α-pinene (4)	0	–	–	–
5	estragole (5)	100	72 (7/8 = 1.6:1.0)	27	n.d.

[a] Reaction conditions: substrate (2 mmol), catalyst (10 mg, 1 μmol of Rh), toluene (20 mL), *P* = 40 atm (CO/H₂ = 1), 80 °C, reaction time 24 h; conversion and selectivity determined by GC. [b] The products of isomerization of limonene, estragole, and β-pinene are terpinolene, anethole, and α-pinene, respectively. [c] Average rate of the substrate conversion (TOF) per mol of the total Rh amount; n.d. not determined.

followed by β-pinene (56% conversion) and limonene (41% conversion). Camphene, also a terminal olefin, showed a much lower reactivity (11% conversion) because of the high steric hindrance of its double bond and gave the corresponding hydroformylation product exclusively (Scheme 4). However, α-pinene, which has an internal double bond, remained virtually intact under the same conditions. Limonene and estragole gave the corresponding aldehydes with ≈70% selectivity, whereas the selectivity for the hydroformylation of β-pinene was only 27%. With these three substrates (limonene, estra-

gole, and β-pinene), their isomerization to give internal olefins (terpinolene, anethole, and α-pinene, respectively) was the only side reaction responsible for the rest of the mass balance. No products of the hydroformylation of internal isomeric olefins were detected in the reaction solutions. Thus, Fe₃O₄@SiO₂-HYP-N(CH₂PPh₂)₂Rh catalyzes the hydroformylation of terminal double bonds successfully but is not active to promote the hydroformylation of internal olefins. Although reaction conditions for each specific substrate could be optimized to improve the catalyst performance, we decided to use estragole as a model substrate to further study the potential of this catalyst for hydroformylation. Our main interests were a comparison with the first-generation material, Fe₃O₄@SiO₂-N(CH₂PPh₂)₂Rh, and to determine the catalyst stability and reusability.

The hydroformylation of estragole gave two main products: the linear and branched aldehydes 7 and 8, respectively (Scheme 5). In addition, the isomerization product anethole (6) was formed in significant amounts; however, only traces of aldehyde 9, which could arise from the hydroformylation of anethole, were detected under the reaction conditions employed.

The data presented in Table 2 were used to compare the performance of the hyperbranched polymer modified catalyst Fe₃O₄@SiO₂-HYP-N(CH₂PPh₂)₂Rh and the unmodified Fe₃O₄@SiO₂-N(CH₂PPh₂)₂Rh material in the hydroformylation of estragole. The reactions were performed with different catalyst loadings (10 and 50 mg, respectively) because of the five-times-higher Rh content in the modified material. The presence of the hyperbranched moieties grafted onto the magnetic support affected the catalytic activity of the solid remarkably. Fe₃O₄@SiO₂-HYP-N(CH₂PPh₂)₂Rh (10 mg) promoted the complete conversion of estragole in 6 h at 80 °C, whereas Fe₃O₄@SiO₂-N(CH₂PPh₂)₂Rh (50 mg) was almost inactive (2% conversion under the same conditions; Table 2, runs 1 and 2). Even at 100 °C, only 14% conversion of estragole was obtained with the unmodified catalyst (Table 2, run 3). Considering that the P/Rh ratio is different in both catalysts, the hyperbranched polymer modified catalyst has a P/Rh ratio of 8, whereas the unmodified catalyst has a P/Rh ratio of 20, a new catalyst was prepared using the hyperbranched polymer modified support with 0.4 wt% of Rh, which corresponds to a P/Rh ratio of 20. This Fe₃O₄@SiO₂-HYP-N(CH₂PPh₂)₂Rh* catalyst (25 mg) also ach-

Table 2. Hydroformylation of estragole (5) catalyzed by Fe₃O₄@SiO₂-N(CH₂PPh₂)₂Rh and Fe₃O₄@SiO₂-HYP-N(CH₂PPh₂)₂Rh.^[a]

Entry	Catalyst	<i>T</i> [°C]	Conversion [%]	Selectivity [%]		TOF ^[b] [h ⁻¹]
				Aldehydes (7/8)	Isomer (6)	
1 ^[c]	Fe ₃ O ₄ @SiO ₂ -HYP-N(CH ₂ PPh ₂) ₂ Rh	80	100	70 (1.9:1.0)	29	540
2 ^[d]	Fe ₃ O ₄ @SiO ₂ -N(CH ₂ PPh ₂) ₂ Rh	80	2	traces	traces	–
3 ^[d]	Fe ₃ O ₄ @SiO ₂ -N(CH ₂ PPh ₂) ₂ Rh	100	14	81 (1.8:1.0)	16	47
4 ^[e]	Fe ₃ O ₄ @SiO ₂ -HYP-N(CH ₂ PPh ₂) ₂ Rh*	80	100	69 (1.9:1.0)	29	1000

[a] Reaction conditions: estragole (2 mmol), toluene (20 mL), *P* = 40 atm (CO/H₂ = 1), reaction time 6 h; conversion and selectivity determined by GC. [b] Initial rate of the substrate conversion (TOF) per mol of the total Rh amount. [c] Catalyst (10 mg, 1 μmol of Rh). [d] Catalyst (50 mg, 1 μmol of Rh). [e] Fe₃O₄@SiO₂-HYP-N(CH₂PPh₂)₂Rh* that contained 0.4 wt% of Rh (25 mg, 1 μmol of Rh) was used in this run.

ieved the complete conversion of estragole in 6 h at 80 °C (Table 2, run 4). Thus, the same amount of Rh in the hyperbranched polymer modified material was much more efficient in the hydroformylation reaction, which implies that the modification of the support with hyperbranched polyester allowed us to increase the number of active species and/or to obtain more active Rh species on the catalyst surface.

Silica-coated magnetic nanoparticles can be attracted uniformly to a permanent magnet and separated efficiently from reaction solutions. The $\text{Fe}_3\text{O}_4@\text{SiO}_2\text{-HYP-N}(\text{CH}_2\text{PPh}_2)_2\text{Rh}$ catalyst was tested in recycling runs after magnetic separation (Table 3). The spent catalyst was recovered magnetically and used in six consecutive reactions, all of which showed a complete conversion without any loss of selectivity (Table 3, runs 1–6). The ratio of the linear and branched aldehydes **7** and **8** in all the runs was approximately 2; that is, the linear isomer accounted for $\approx 70\%$ of the aldehyde product. The reaction solutions after runs 1–6 (Table 3) were analyzed by using ICP-OES, and no Rh was detected within the detection

limit of the equipment. Moreover, after the catalyst removal in the first and sixth reaction cycles, fresh estragole was added to the supernatants. The reactions were allowed to proceed further, and no additional substrate conversion was observed (Table 3, runs 7 and 8). Notably, the catalyst was exposed to air during each recovery procedure in the recycling runs and did not deactivate, which demonstrates its high air stability.

Next, the hydroformylation of estragole was monitored by taking aliquots at different time intervals for GC analysis (Table 4). The kinetic curve for the reaction with the fresh catalyst (first reaction cycle) showed a clearly pronounced induction period: 27% conversion in the first and 89% in the second hour of reaction (Table 4, run 1). The reaction was accelerated by an increase of the hydrogen partial pressure (Table 4, run 2 vs. run 1) and decelerated by CO (Table 4, run 3 vs. run 1). However, neither an increase of the hydrogen or CO concentration eliminated the induction period. The kinetic monitoring of the second and third reaction cycles revealed not only the shortness of the induction period (if any) but also

Table 3. Hydroformylation of estragole (**5**) catalyzed by $\text{Fe}_3\text{O}_4@\text{SiO}_2\text{-HYP-N}(\text{CH}_2\text{PPh}_2)_2\text{Rh}$: recycling.^[a]

Entry	Reaction cycle	t [h]	Conversion [%]	Selectivity [%]	
				Aldehydes (7/8)	Isomer (6)
1	1st	6	100	70 (1.9:1.0)	29
2 ^[b]	2nd	6	100	72 (1.9:1.0)	27
3 ^[b]	3rd	6	100	73 (1.8:1.0)	26
4 ^[b]	4th	3	100	66 (2.0:1.0)	32
5 ^[b]	5th	3	100	72 (1.9:1.0)	27
6 ^[b]	6th	3	100	71 (1.8:1.0)	28
7 ^[c]	supernatant after run 1	6	0	–	–
8 ^[c]	supernatant after run 6	6	0	–	–

[a] Reaction conditions: estragole (2 mmol), catalyst (10 mg, 1 μmol of Rh), toluene (20 mL), $P=40$ atm ($\text{CO}/\text{H}_2=1$), 80 °C; conversion and selectivity determined by GC. [b] The spent catalyst recycled after run 1 was used in these runs. [c] After runs 1 and 6, respectively, the catalyst was removed magnetically (and was used in recycling experiments), fresh estragole (2 mmol) added and the reaction was allowed to proceed; no further conversion was observed.

Table 4. Hydroformylation of estragole (**5**) catalyzed by $\text{Fe}_3\text{O}_4@\text{SiO}_2\text{-HYP-N}(\text{CH}_2\text{PPh}_2)_2\text{Rh}$.^[a]

Entry	P_{CO} [atm]	P_{H_2} [atm]	t [h]	Conversion [%]	Selectivity [%]		TOF ^[b] [h^{-1}]
					Aldehydes (7/8)	Isomer (6)	
1	20	20	1	27	69 (1.9:1.0)	30	540
			2	89	70 (1.9:1.0)	29	
			3	100	70 (1.9:1.0)	30	
2	20	40	0.5	35	77 (1.7:1.0)	23	1400
			1	87	78 (1.7:1.0)	22	
			2	100	78 (1.7:1.0)	22	
3	40	20	0.5	0	–	–	360
			1	18	68 (1.9:1.0)	30	
			2	49	69 (1.9:1.0)	30	
4 ^[c]	20	20	2.5	65	70 (1.9:1.0)	29	880
			1	44	68 (1.9:1.0)	31	
			2	98	69 (1.9:1.0)	29	
5 ^[c]	20	20	3	100	70 (1.9:1.0)	29	1480
			1	74	69 (1.9:1.0)	30	
			2	100	68 (1.9:1.0)	29	
			3	100	70 (1.9:1.0)	28	

[a] Reaction conditions: estragole (2 mmol), catalyst (10 mg, 1 μmol of Rh), toluene (20 mL), 80 °C; conversion and selectivity were determined by GC. [b] Initial rate of substrate conversion (turnover frequency) per mol of the total Rh amount. [c] The spent catalyst recycled after run 1 was consequently used in run 4 (2nd reaction cycle) and then in run 5 (3rd reaction cycle).

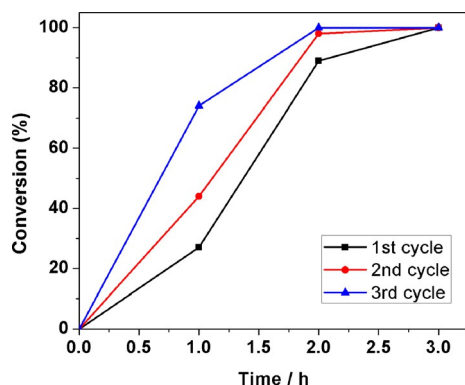


Figure 3. Hydroformylation of estragole catalyzed by $\text{Fe}_3\text{O}_4@SiO_2\text{-HYP-N}(\text{CH}_2\text{PPh}_2)_2\text{Rh}$: recycling experiments. Conditions: estragole (2 mmol), catalyst (10 mg, 1 μmol of Rh), toluene (20 mL), 40 atm (CO/H_2) = 1, 80 °C. Conversion of 100% corresponds to a turnover number of 2000.

the remarkable increase in the catalyst activity, expressed by the turnover frequency (TOF), after each recovery procedure (Table 4, cf. runs 1, 4, and 5; Figure 3). Thus, it can be suggested that during the first reaction cycle active catalytic species are formed from the Rh precursor on the catalyst surface. Such activation could occur through the corrosive chemisorption of Rh NPs in the presence of CO.^[25] The formation of relatively strong Rh–CO bonds and the weakening of the Rh–Rh bonds could result in the appearance of molecular Rh species immobilized on the solid surface by the interaction with phosphine ligands grafted on the silica matrix. Notably, no changes in the regio- and chemoselectivity of the reaction were observed in the recycling experiments (Tables 3 and 4), which indicates that the nature of the catalytically active species remains essentially unchanged.

In the recycling experiments, an increase in the TOF was observed (Table 4, cf. run 1, 4, and 5; Figure 3) in the successive reactions even though the catalyst was not protected from air during the recovery procedure. However, we still need to investigate the stability of the diphenylphosphine ligand that can be partially oxidized under exposure to air. The Raman spectra of the diphenylphosphine ligand, free and grafted onto the support before and after reaction, are shown in Figure 4. Notably, the Raman spectrum obtained from the diphenylphosphine ligand grafted onto the support exhibits the characteristic Raman bands of the phosphine ligand, which contrasts the behavior of the analogous catalysts prepared without the hyperbranched polymer strategy^[15] and suggests a more efficient phosphine grafting in the silica matrix. Additionally, these results provide a clear indication of the phosphine functionalization on the $\text{Fe}_3\text{O}_4@SiO_2$ support, which was not possible to access through FTIR spectroscopy because of the different selectivity of these vibrational techniques.

The ordinary Raman spectrum of HPPH_2 is shown in Figure 4a. The spectrum was dominated by the bands at $\tilde{\nu}=618$ (phenyl ring in-plane deformation), 687 (phenyl ring out-of-plane deformation), 800 (phenyl C–H out-of-plane deformation), 999 (phenyl ring breathing), 1028 (phenyl C–H in-plane deformation), 1100 (P–C ring stretching), and 1585 cm^{-1} (Ph

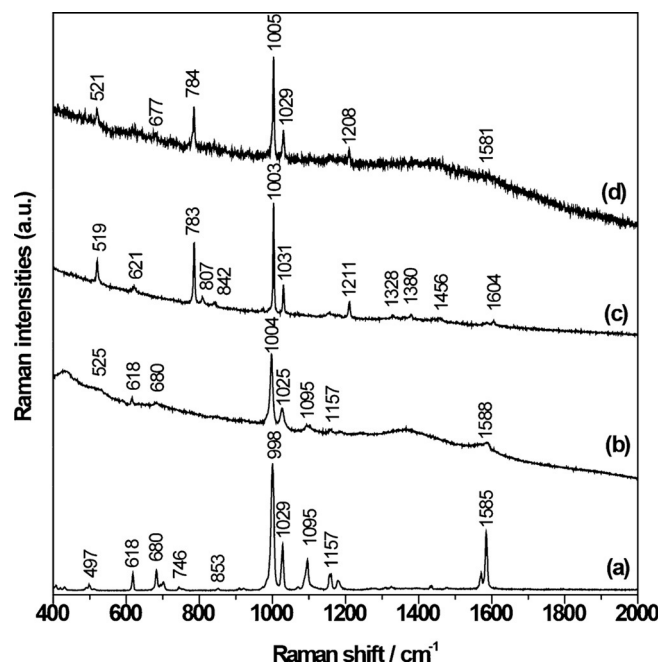


Figure 4. Raman spectra of a) diphenylphosphine, b) $\text{Fe}_3\text{O}_4@SiO_2\text{-HYP-N}(\text{CH}_2\text{PPh}_2)_2$, c) $\text{Fe}_3\text{O}_4@SiO_2\text{-HYP-N}(\text{CH}_2\text{PPh}_2)_2\text{Rh}$ catalyst before the reaction, and d) $\text{Fe}_3\text{O}_4@SiO_2\text{-N}(\text{CH}_2\text{PPh}_2)_2\text{Rh}$ catalyst after the reaction. Data were collected at $\lambda_{\text{exc}} = 632.8$ nm.

C–C stretching).^[24] The Raman spectrum of $\text{Fe}_3\text{O}_4@SiO_2\text{-HYP-N}(\text{CH}_2\text{PPh}_2)_2$ (exposed to air) is shown in Figure 4b. The main bands that correspond to the diphenylphosphine ligand were observed at $\tilde{\nu}=1004$ (phenyl ring breathing) and 1588 cm^{-1} (Ph C–C stretching), but there was no clear evidence of ligand oxidation. The main difference in the Raman spectra of diphenylphosphine before and after oxidation (exposure to air) is the appearance of a new band at $\tilde{\nu}=1181$ cm^{-1} (P=O stretching mode),^[17] which was not present in the spectrum shown in Figure 4b. After the immobilization of Rh NPs on $\text{Fe}_3\text{O}_4@SiO_2\text{-HYP-N}(\text{CH}_2\text{PPh}_2)_2$ (Figure 4c), the Raman spectrum exhibited changes in both intensity and band positions that were attributed to the interaction between phosphine ligands and the metallic NPs.^[17,26] The main evidence for ligand–metal interactions was the enhancement of the Ph–X-sensitive mode at approximately $\tilde{\nu}=519$ cm^{-1} and the enhancement of the band at $\tilde{\nu}=783$ cm^{-1} assigned to the phenyl C–H out-of-plane deformation. The presence of the band at $\tilde{\nu}=1211$ cm^{-1} could suggest the oxidation of the diphenylphosphine ligand during the immobilization of the Rh NPs (it was attributed previously to an enhancement of the P=O stretching mode),^[17] but this band can also be attributed to an enhancement of the phenyl ring C–H in-plane deformation mode. Notably, the three bands at $\tilde{\nu}=519$, 783, and 1211 cm^{-1} may be a signature of the adsorption of a phosphine moiety on the metallic NPs as they were not observed if Rh^{3+} ions interact with phosphine ligands.^[20] The Raman spectrum of the spent catalyst after the hydroformylation reaction (Figure 4d) exhibits the main bands attributed to the interaction of the diphenylphosphine ligand with the metallic NPs (mainly the bands at $\tilde{\nu}=521$, 784, and 1208 cm^{-1}), which suggests that Rh NPs still interact with the ligands graft-

ed on the support. This result is in agreement with the TEM analysis that shows the presence of Rh NPs at the support surface of the used catalyst (Figure S4). The intensity of the band at $\tilde{\nu} = 1208 \text{ cm}^{-1}$ decreased, but this was also the case for the other phenyl ring modes, which makes it difficult to ascertain if this decrease in intensity is because of the reduction of the diphenylphosphine oxide under the reaction conditions or is a consequence of the decrease of the number of supported metal NPs. If we consider that the Rh NPs are the precursors of the active molecular species formed in situ as suggested before,^[25] a decrease in the number of Rh NPs on the support through their corrosive chemisorption in the presence of CO is expected. The vibrational mode associated with P–C ring stretching in the grafted ligand at $\tilde{\nu} = 1095 \text{ cm}^{-1}$ (Figure 4b) was no longer observed after the immobilization of Rh NPs on $\text{Fe}_3\text{O}_4@\text{SiO}_2\text{-HYP-N}(\text{CH}_2\text{PPh}_2)_2$ (Figure 4c) or in the spent catalyst (Figure 4d), which does not allow us to draw conclusions about the interaction between P and the Rh surface.

Conclusions

The functionalization of silica-coated magnetite with a hyperbranched polymer was used as a strategy to enhance the number of terminal phosphine groups available to interact with a Rh catalyst prepared through the immobilization of Rh nanoparticles (NPs) onto the support surface. This strategy enhanced the number of terminal phosphine groups and, consequently, improved the metal–support interaction, the metal loading on the support (up to 1 wt% Rh), and the catalytic activity. This new catalyst contains five times more metal than a previous example prepared by the direct phosphinomethylation of the silica surface functionalized with (3-aminopropyl)triethoxysilane. The synthesis enabled the preparation of an air-stable, easily recovered, and reusable catalyst for the hydroformylation of substrates obtained from essential oils of many plants that represent a green alternative source of renewable feedstocks for the flavor and fragrance industry. The Raman data obtained suggested that Rh NPs still interact with the ligands grafted on the support after the first reaction cycle, but it does not exclude the presence of molecular species adsorbed on the catalyst support. Solid-state ^{31}P NMR spectroscopy and X-ray photoelectron spectroscopy were not conclusive for the characterization of the catalyst, and further experiments using unsupported Rh NPs are in progress.

Experimental Section

Materials

Trimethylolpropane (TMP), 2,2-bis(hydroxymethyl)propionic acid (bis-MPA), *p*-toluenesulfonic acid monohydrate (*p*-TSA), 4-(dimethylamino)pyridine (DMAP), glycine (Gly), glutaraldehyde, dicyclohexylcarbodiimide (DCC), BOC, trifluoroacetic acid (TFA), TOAB, rhodium(III) chloride hydrate, sodium borohydride, and silica gel for chromatography (pore size 60 Å, 220–440 mesh particle size) were purchased from Sigma–Aldrich (St. Louis, MO). All HPLC-grade solvents utilized were obtained from EMD Millipore (Billerica, MA). Deuterated DMSO ($[\text{D}_6]\text{DMSO}$), deuterated methanol

($[\text{D}_4]\text{MeOD}$), and deuterated chloroform (CDCl_3) were purchased from Cambridge Isotope Laboratories (Tewksbury, MA). Deionized (DI) water (resistivity of $18.2 \text{ M}\Omega \text{ cm}^{-1}$) was obtained by using a NANOpure Diamond UV ultrapure water system (Barnstead International, Lake Balboa, CA). Toluene for the hydroformylation reaction was dried with sodium wire and benzophenone under reflux for 8 h and then distilled under Ar.

Preparation of Rh NPs

Rh NPs were synthesized as reported elsewhere.^[24] Rhodium(III) chloride hydrate (30 mg, 0.11 mmol of Rh) and TOAB (130 mg, 0.23 mmol) were dissolved in DI water (30 mL) and toluene (30 mL), respectively, at RT. The aqueous phase was adjusted to pH 6 by the addition of aqueous NaOH. The phase-transfer reagent solution was added dropwise to the RhCl_3 aqueous solution, and the mixture was stirred for 30 min. An aqueous sodium borohydride solution (5 mL, 1.36 mmol) was prepared freshly and added dropwise to the mixture. The organic layer turned black, and the system was further stirred for 3 h. Then, the organic phase that contained the Rh NPs was separated and washed twice with DI water. The NPs synthesized by this procedure were referred to as Rh-TOAB NPs.

Preparation of the catalyst support

The catalyst support consists of silica-coated magnetite NPs ($\text{Fe}_3\text{O}_4@\text{SiO}_2$) prepared by a reverse microemulsion method described elsewhere.^[26] A calcination step (2 h at 540°C) was applied to remove any organic residues and resulted in an increase of the surface area from ≈ 20 to $100 \text{ m}^2 \text{ g}^{-1}$. The silica surface was modified with terminal amino groups using (3-aminopropyl)triethoxysilane. The solid (200 mg) was added to the (3-aminopropyl)triethoxysilane solution (1% v/v) in dry toluene (200 mL) under a N_2 atmosphere. The mixture was stirred at RT for 2 h, and the solid was separated magnetically. The material, $\text{Fe}_3\text{O}_4@\text{SiO}_2\text{-NH}_2$, was washed twice with toluene and acetone and dried at 100°C for 20 h.

Synthesis of hyperbranched polymer HYP-[G#2]-(OH)₁₂

TMP (5.55 mmol, 0.745 g) and *p*-TSA (33.6 mg, 0.5 wt% of bis-MPA) were mixed carefully in a round-bottomed three-necked flask equipped with a dry N_2 inlet, a drying tube, and a mechanical stirrer. The flask was placed in an oil bath heated to 140°C . The mixture was left to react under a stream of dry N_2 . Then, through an addition funnel for solids, bis-MPA (50 mmol, 6.71 g; stoichiometric amount for a perfect second-generation material) was added portionwise to the mixture. The N_2 stream was kept to remove the water formed in the reaction. After 2 h of addition, the flask was sealed and connected to a vacuum line and the pressure was reduced ($12 \text{ mm}_{\text{Hg}}$) overnight. After the equalization of the pressure in the flask, the resulting material, HYP-[G#2]-(OH)₁₂, was stored under anhydrous conditions. ^1H NMR (200 MHz, $[\text{D}_6]\text{DMSO}$): $\delta = 0.82$ (t, 3H, $-\text{CH}_3$), 1.02 (s, 20H, $-\text{CH}_3$), 1.07 (s, 36H, $-\text{CH}_3$), 1.17 (s, 12H, $-\text{CH}_3$), 3.42–3.48 (m, 52H, $-\text{CH}_2$), 4.06–4.12 (m, 38H, $-\text{CH}_2$), 4.62 (s, 12H, $-\text{OH}$), 4.94 ppm (s, 11H, $-\text{OH}$); ^{13}C NMR (50 MHz, $[\text{D}_6]\text{DMSO}$): $\delta = 7.3$, 16.8, 17.3, 22.4, 41.0, 46.4, 50.3, 63.7, 64.5, 172.0, 174.1 ppm.

Synthesis of dendrimer HYP-[G#2]-(NH₂)_z

Preparation of Glycine-Boc adduct (Gly-Boc)

Glycine (5.0 g, 66.6 mmol) was suspended in a mixture of dioxane (40 mL) and a solution NaOH (40 mL, 1 mol L⁻¹) in an ice bath. BOC (15.99 g, 16.83 mL, 73.26 mmol) was added dropwise to the solution, and the reaction was stirred at RT for 8 h. The organic solvent was removed under vacuum, and the pH of the resulting aqueous phase was adjusted to 4 by the addition of a 1 mol L⁻¹ solution of HCl. The aqueous layer was extracted with EtOAc (3 × 100 mL). The organic phase was dried with MgSO₄ and concentrated and dried under vacuum to give Gly-BOC as a white powder (95%). ¹H NMR (200 MHz, CDCl₃): δ = 1.46 (s, 6H, -CH₃), 1.53 (s, 3H, -CH₃), 3.97 ppm (d, 2H, -CH₂).

Preparation of HYP-[G#2]-(Gly-BOC)_y

HYP-[G#2]-(OH)₁₂ (2.5 g, 2.12–25.44 mmol of OH-1 equiv.), Gly-BOC (5.79 g, 33.07 mmol, 1.3 equiv.), DMAP (4.04 g, 33.07 mmol, 1.3 equiv.), and pyridine (10.3 mL, 127.2 mmol, 5 equiv.) were dissolved in dry CH₂Cl₂ (50 mL) in an ice bath. A solution of DCC (6.82 g, 33.07 mmol, 1.3 equiv.) in CH₂Cl₂ (25 mL) was then added dropwise. The mixture was warmed to RT and left to react for 72 h. The urea formed and the unreacted catalyst were removed by filtration. The filtrate was diluted in CH₂Cl₂ (1 L), and the organic phase was washed with a 10% w/w solution of NaHSO₄ (3 × 120 mL) and brine (1 × 120 mL). The organic phase was dried with MgSO₄, concentrated, and dried under vacuum. The residue was purified by liquid column chromatography on silica gel, eluting with a 60:40 mixture of EtOAc/hexane to give HYP-[G#2]-(Gly-BOC)_y as a yellow oil (82%). ¹H NMR (200 MHz, CDCl₃): δ = 0.88 (t, 3H, -CH₃), 1.26 (m, 27H, -CH₃), 1.44 (s, 81H, -CH₃), 3.89 (d, 20H, -CH₂), 4.10 (s, 6H, -CH₂), 4.27 (s, 36H, -CH₂), 5.38 ppm (s, 9H, -NH). ¹³C NMR (50 MHz, [D₆]DMSO): δ = 17.2, 17.3, 17.6, 50.6, 50.7, 63.6, 64.2, 64.2, 64.4, 65.3, 68.5, 68.8, 70.2, 70.3, 172.9, 174.5, 174.7, 175.1 ppm; HRMS (ESI): *m/z*: calcd for C₁₁₄H₁₈₅N₉O₅₇: 2612.16 [*M*+Na⁺]; found: 2616.10.

Preparation of HYP-[G#2]-(NH₂)_z

HYP-[G#2]-(Gly-BOC)_y (2.0 g, 0.65 mmol) was dissolved in CH₂Cl₂ (5 mL) in an ice bath, then TFA (5 mL) and CH₂Cl₂ (1:1) were added dropwise. The mixture was warmed to RT and stirred for 15 min. The solvent and residual acid were removed by vacuum. The residue, HYP-[G#2]-(NH₂)_z, was then stirred in the presence of ion-exchange resin (2 g; Amberlyst, hydroxide form) in dry methanol (10 mL) for 15 min. ¹H NMR (200 MHz, [D₄]MeOD): δ = 0.99 (t, 3H, -CH₃), 1.21 (s, 9H, -CH₃), 1.33 (m, 18H, -CH₃), 1.60 (q, 2H, -CH₂), 3.92 (d, 7H, -CH₂), 4.16 (s, 6H, -CH₂), 4.31–4.43 ppm (m, 36H, -CH₂); ¹³C NMR (50 MHz, [D₆]DMSO): δ = 16.9, 17.5, 39.9, 46.7, 50.6, 50.8, 52.6, 64.1, 64.8, 66.7, 168.4, 173.3, 174.6 ppm; HRMS (ESI): *m/z*: calcd for C₇₃H₁₁₉N₁₁O₄₁: 1827.42 [*M*+Na⁺]; found: 1834.84.

Preparation of Fe₃O₄@SiO₂-HYP-N-(CH₂PPh₂)₂

Preparation of Fe₃O₄@SiO₂-HYP-NH₂

In a round-bottomed flask, Fe₃O₄@SiO₂-NH₂ (200 mg; 9.4 μmol of NH₂) was suspended in a phosphate buffer solution (PBS; 40 mL; pH 7.2, 0.1 mol L⁻¹) with a mechanical stirrer. A glutaraldehyde aqueous solution (1.6 mL, 50 wt% in water) was added, and the mixture was stirred vigorously at RT for 1.5 h. The aldehyde-func-

tionized nanoparticles were isolated by centrifugation and washed several times with PBS and water. The material was kept in aqueous medium before use. HYP-[G#2]-(NH₂)_z (4.59 g, 2.81 mmol, 3 equiv.) was dissolved in PBS (200 mL, pH 7.2, 0.1 M). Aldehyde-functionalized nanoparticles (2.0 g, 0.94 mmol of terminal aldehyde, 1 equiv.) were then suspended in PBS (200 mL) and added to the first suspension portionwise. The mixture was left to react at RT overnight. The modified nanoparticles were isolated by centrifugation and washed several times with PBS and water. Finally the solid product Fe₃O₄@SiO₂-HYP-NH₂ was washed with methanol and kept in this organic medium.

Preparation of Fe₃O₄@SiO₂-HYP-N(CH₂PPh₂)₂

The terminal amino groups in Fe₃O₄@SiO₂-HYP-NH₂ were subjected to phosphinomethylation.^[21] Under an inert atmosphere (N₂), a mixture of paraformaldehyde (1.82 mmol) and diphenylphosphine (2.00 mmol) in methanol (5 mL) was heated at 60 °C for 1 h. Then, the suspension of Fe₃O₄@SiO₂-HYP-NH₂ (1.00 g, 0.5 mmol of -NH₂) in a toluene (20 mL)/methanol (10 mL) solution was added to the reaction mixture, which was stirred overnight at RT. Then, the solid, Fe₃O₄@SiO₂-HYP-N(CH₂PPh₂)₂, was washed five times with toluene and dried under vacuum.

Preparation of Fe₃O₄@SiO₂-HYP-N(CH₂PPh₂)₂Rh

Fe₃O₄@SiO₂-HYP-N(CH₂PPh₂)₂ was used as the support for the immobilization of Rh NPs. A toluene solution that contained Rh-TOAB NPs (≈30 mL, 0.11 mmol of Rh) was added to the support (500 mg). The mixture was stirred overnight, and the solids were separated magnetically. After the separation, the catalyst, Fe₃O₄@SiO₂-HYP-N(CH₂PPh₂)₂Rh, was washed several times with toluene and dried under vacuum.

Catalytic reactions

Catalytic experiments were performed in 100 mL homemade stainless-steel reactors with magnetic stirring. Reactions were followed by using GC by sampling the liquid phase with a valved dip tube. Typically, a mixture of toluene (20 mL), the Rh catalyst (10 mg, 1 μmol of Rh), the substrate (2.0 mmol), and dodecane (internal standard, 1 mmol) was transferred to the reactor, which was pressurized to 40–60 atm with a CO/H₂ mixture. The temperature (80–100 °C) was maintained with an oil bath and a hot-stirring plate connected to a digital temperature controller. The reactions were conducted under magnetic stirring (700 rpm). After the reaction was performed, the reactor was cooled to RT, the pressure was released, and the catalyst was recovered magnetically with an external magnet.

Characterization methods

TEM was performed by using a Jeol-2100 microscope. Samples for TEM were prepared by placing a drop that contained the nanoparticles dispersed in propan-2-ol on a carbon-coated copper grid (Ted Pella, Inc.). The Rh content in the catalysts was measured by using FAAS by using a Shimadzu AA-6300 Atomic Absorption Spectrophotometer. The Rh leaching to the supernatant solutions was measured by using a SPECTO ARCOS ICP-OES. The products were analyzed by using GC (Shimadzu QP2010 GC, Rtx-5MS capillary column, flame ionization detector (FID)) and GC-MS (Shimadzu QP2010-PLUS instrument operating at 70 eV). The conversion and

selectivity were determined by using GC. The GC mass balance was based on the substrate charged using dodecane as an internal standard. Raman spectra were acquired by using a Renishaw Raman InVia equipped with a charge coupled device (CCD) detector and coupled to a Leica microscope, which allowed the rapid accumulation of Raman spectra with a spatial resolution of ≈ 1 mm (micro-Raman technique). The laser beam was focused on the sample by using a $50\times$ lens. The laser power was always kept below 0.7 mW at the sample. The experiments were performed under ambient conditions using a back-scattering geometry. The samples were irradiated with the $\lambda = 632.8$ nm line of a He-Ne laser (Renishaw RL633 laser).

Acknowledgements

The authors are grateful to INCT-Catalise and the Brazilian government agencies FAPESP, CNPq, and FAPEMIG for financial support.

Keywords: heterogeneous catalysis · hydroformylation · nanoparticles · rhodium · supported catalysts

- [1] L. M. Rossi, N. J. S. Costa, F. P. Silva, R. Wojcieszak, *Green Chem.* **2014**, *16*, 2906–2933.
- [2] A. F. Cardozo, E. Manoury, C. Julcour, J.-F. Blanco, H. Delmas, F. Gayet, R. Poli, *ChemCatChem* **2013**, *5*, 1161–1169.
- [3] S. Shylesh, D. Hanna, S. Werner, A. T. Bell, *ACS Catal.* **2012**, *2*, 487–493.
- [4] a) N. J. S. Costa, L. M. Rossi, *Nanoscale* **2012**, *4*, 5826–5834; b) A. Corma, H. Garcia, *Adv. Synth. Catal.* **2006**, *348*, 1391–1412.
- [5] S. C. Bourque, F. Maltais, W.-J. Xiao, O. Tardif, H. Alper, P. Arya, L. E. Manzer, *J. Am. Chem. Soc.* **1999**, *121*, 3035–3038.
- [6] C. Gao, D. Yan, *Prog. Polym. Sci.* **2004**, *29*, 183–275.
- [7] G. V. Korolev, M. L. Bubnova, *Polym. Sci. Ser. C* **2007**, *49*, 332–354.
- [8] a) B. Voit, *J. Polym. Sci. Part A* **2005**, *43*, 2679–2699; b) D. E. Bergbreiter, J. Tian, C. Hongfa, *Chem. Rev.* **2009**, *109*, 530–582; c) D. E. Bergbreiter, *ACS Macro Lett.* **2014**, *3*, 260–265.
- [9] C. J. Stephenson, J. P. McInnis, C. Chen, M. P. Weberski, A. Motta, M. Delferro, T. J. Marks, *ACS Catal.* **2014**, *4*, 999–1003.
- [10] Y. Nabae, J. Liang, X. Huang, T. Hayakawa, M.-a. Kakimoto, *Green Chem.* **2014**, *16*, 3596–3602.
- [11] a) E. B. Hager, B. C. E. Makhubela, G. S. Smith, *Dalton Trans.* **2012**, *41*, 13927–13935; b) L. Tuchbreiter, S. Mecking, *Macromol. Chem. Phys.* **2007**, *208*, 1688–1693; c) A. Gong, Q. Fan, Y. Chen, H. Liu, C. Chen, F. Xi, *J. Mol. Catal. A* **2000**, *159*, 225–232.
- [12] S.-M. Lu, H. Alper, *J. Am. Chem. Soc.* **2003**, *125*, 13126–13131.
- [13] B. Helms, J. M. J. Fréchet, *Adv. Synth. Catal.* **2006**, *348*, 1125–1148.
- [14] a) P. Li, S. Kawi, *J. Catal.* **2008**, *257*, 23–31; b) C. Bianchini, P. Barbaro, *Top. Catal.* **2002**, *19*, 17–32.
- [15] T.-J. Yoon, J. I. Kim, J.-K. Lee, *Inorg. Chim. Acta* **2003**, *345*, 228–234.
- [16] R. Abu-Reziq, H. Alper, D. Wang, M. L. Post, *J. Am. Chem. Soc.* **2006**, *128*, 5279–5282.
- [17] M. A. S. Garcia, K. C. B. Oliveira, J. C. S. Costa, P. Corio, E. V. Gusevskaya, E. N. dos Santos, L. M. Rossi, *ChemCatChem* **2015**, *7*, 1566–1572.
- [18] E. Malmstroem, M. Johansson, A. Hult, *Macromolecules* **1995**, *28*, 1698–1703.
- [19] a) N. Chauhan, J. Narang, Sunny, C. S. Pundir, *Enzyme Microb. Technol.* **2013**, *52*, 265–271; b) L. Rossi, A. Quach, Z. Rosenzweig, *Anal. Bioanal. Chem.* **2004**, *380*, 606–613.
- [20] J. Huang, H. Wang, D. Li, W. Zhao, L. Ding, Y. Han, *Mater. Sci. Eng. C* **2011**, *31*, 1374–1378.
- [21] M. T. Reetz, G. Lohmer, R. Schwickardi, *Angew. Chem. Int. Ed. Engl.* **1997**, *36*, 1526–1529; *Angew. Chem.* **1997**, *109*, 1559–1562.
- [22] A. M. Vaz, D. Serrano-Ruiz, M. Laurenti, P. Alonso-Cristobal, E. Lopez-Cabarcos, J. Rubio-Retama, *Colloids Surf. B* **2014**, *114*, 11–19.
- [23] M. Brust, M. Walker, D. Bethell, D. J. Schiffrin, R. Whyman, *J. Chem. Soc. Chem. Commun.* **1994**, 801–802.
- [24] L. M. Rossi, L. L. R. Vono, M. A. S. Garcia, T. L. T. Faria, J. A. Lopez-Sanchez, *Top. Catal.* **2013**, *56*, 1228–1238.
- [25] S. Shylesh, D. Hanna, A. Mlinar, X.-Q. Kōng, J. A. Reimer, A. T. Bell, *ACS Catal.* **2013**, *3*, 348–357.
- [26] M. J. Jacinto, P. K. Kiyohara, S. H. Masunaga, R. F. Jardim, L. M. Rossi, *Appl. Catal. A* **2008**, *338*, 52–57.

Received: January 20, 2016

Published online on May 12, 2016